Experimental Performance of a Passively Driven Displacer

H. Rana, M. Dadd, M. A. Abolghasemi, P. Bailey, R. Stone

Department of Engineering Science, University of Oxford
Oxford, OX1 3PJ

ABSTRACT

Stirling pulse tube cryocoolers (SPTCs) incorporate a warm end displacer into a pulse tube cryocooler. Previous studies have demonstrated that an active displacer integrated into an SPTC yields good performance and better efficiencies than pulse tube cryocoolers with inertance tubes. Using an active displacer that is driven by a motor requires a second phase from the power electronics. This results in an increased complexity of the design due to the extra motor and electrical feedthrough; hence it is preferable to have a passively driven displacer. This study presents the experimental testing and validation of a passively driven displacer integrated within a coaxial Stirling pulse tube cryocooler. The pressure and harmonic driving forces of the displacer are analyzed and a validation of the displacer operation is presented with the theoretically modelled passive displacer.

INTRODUCTION

Stirling pulse tube cryocoolers (SPTCs) provide active cooling for detectors and other electronic devices to cryogenic temperatures. They are compact and efficient, making them a favorable cryocooler solution for spaceflight missions. The SPTC efficiency and performance is governed by the intricate interplay between the mass flow and pressure pulse throughout the pulse tube, which can be controlled by orifices, inertance tubes, and displacers at the warm end [1]. SPTCs employing active displacers have been reported to reach higher efficiencies than other phase control methods, due to their ability to recover expansion (PV) power at the warm end back into the system [2]. However, the use of an active displacer results in a more complex design in order to integrate the second motor and introduces a second phase from the power electronics into the system [3]. Hence, removing the second motor requirement and being able to run the displacer passively is preferable [4].

A coaxial SPTC with a passive warm end displacer has been built and tested. Inputs from the coaxial configuration SPTC with an active displacer were utilized as starting baselines for the design of the passive displacer SPTC, where the additional motor was removed and a harmonic design was completed for the displacer [5]. This paper reports on the experimental build and testing of the passive displacer operation and validation of its activity with the designed components and full assembly. The flexure springs for use in the displacer were stiffness tested and fatigue tested and the fully assembled displacer was run in clamped and dynamic tests to investigate the pressure and harmonic forces driving the system.

Cryocoolers 22, edited by R.G. Ross, Jr., J.R. Raab and S.D. Miller

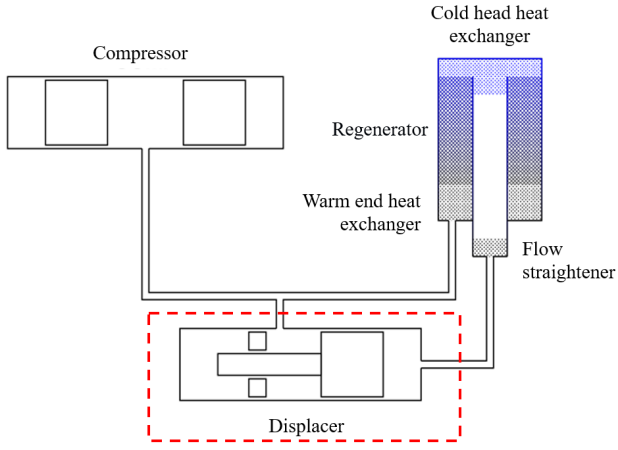

Figure 1. The coaxial Stirling pulse tube cryocooler design where the warm end displacer is indicated.

PASSIVE DISPLACER DESIGN

Displacer Design

Figure 1 presents a schematic of the coaxial SPTC design where the warm end displacer is highlighted. The pulse tube is positioned within the coaxial regenerator and the displacer operates at the warm end in order to create a phase difference with the compressor motion, and in turn, generate a phase lag between the mass flow and pressure pulse throughout the pulse tube assembly. The compressor unit features a dedicated motor to run the compressor drive, and in the case of the passive design explored in this study, no motor is used at the warm end displacer.

Harmonic and Pressure Driving Forces

The passive displacer is driven by the pressure difference that is generated across its back and front ends during SPTC operation. The pressure and harmonic forces that run the displacer require defining and balancing in order to reconstruct and simulate its operation. Figure 2 shows the mechanical schematic for the passive displacer, where the displacer piston, flexure springs and moving mass are indicated. Furthermore, the regions over which the different pressure forces act during operation are indicated.

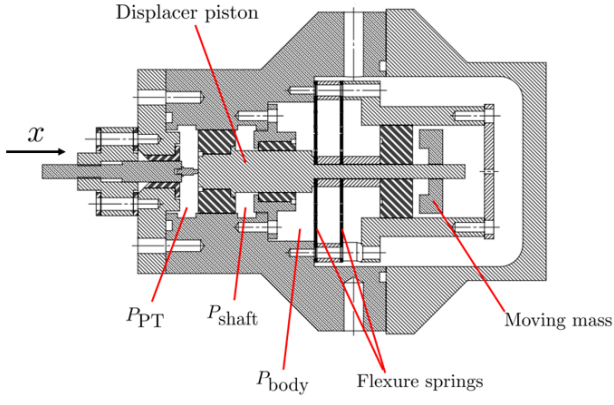

Figure 2. Mechanical schematic for the passive displacer where the areas over which the driving pressure forces act are indicated. The contact probe shown to the left of the displacer was later replaced with an optical window and an Omron laser displacement transducer was installed for displacement measurements.

The sinusoidal displacement and pressure waveform can be given as per Equations 1 and 2.

$$x_d = x_o \sin(\omega t + \phi_d) \tag{1}$$

$$P = P_{b,f} \cos(\omega t + \phi_{b,f}) \tag{2}$$

Taking the differential of Equation 1 gives the velocity from which the damping force can be derived and differentiating again allows calculation of the inertial force. The pressure forces and the harmonic forces can be equated for the passive displacer, as given by Equation 3.

$$\underbrace{P_{body}A_{shaft}}_{F_{inlet}} + \underbrace{(A_{PT} - A_{shaft})\,P_{shaft}}_{F_{body}} - \underbrace{P_{PT}A_{PT}}_{F_{PT}} = \underbrace{-cx_o\omega \cos(\omega t + \phi_d)}_{F_{damping}} - \underbrace{(k - m\omega^2)(x_o \sin(\omega t + \phi_d))}_{F_{spring}\ F_{inertial}} \tag{3}$$

When these forces are in balance, the displacer is able to run passively, and hence the harmonic design for the pressure-driven displacer is achieved.

Flexure Springs Analysis and Testing

The flexure springs, as indicated in Figure 2, form a key part of the harmonic design of the passive displacer. Their design for this displacer assembly has previously been reported, where FE analysis was completed to ascertain the spring stiffness and fatigue limit for designed springs, and further, the stiffness and moving mass were experimentally validated [5]. In this study, the springs were experimentally fatigue tested, where two different designs A and B, each produced by two different manufacturers X and Y, were investigated. The experimental testing setup is a low cost flexure testing assembly that permits 'fail safe' continuous fatigue testing [6]. All springs were 30 mm in diameter with an 8 mm design stroke. Figure 3 presents the fatigue test results for design A and Figure 4 shows design B, where the data in blue represents the springs made by manufacturer X and the data in red are by manufacturer Y. The cumulative number of oscillatory cycles of the spring motion (as a function of the drive frequency) is presented against the stroke at which the spring is being run. The stroke was incrementally increased once 10^7 cycles had been completed

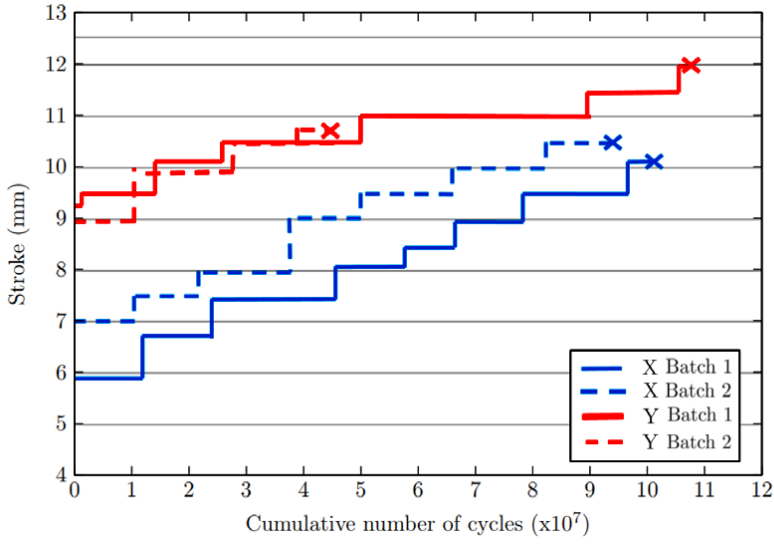

Figure 3. Fatigue performance of spring design A, were springs of 0.3 mm by manufacturers X and Y were tested. The 'x' indicates failure occurred.

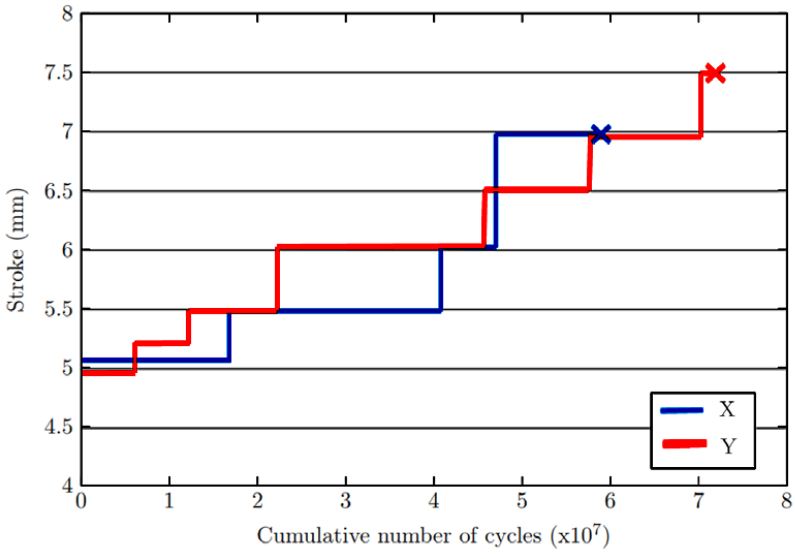

Figure 4. Fatigue plot for spring design B, where springs of 0.3 mm by manufacturers X and Y were tested. The 'x' indicates failure occurred.

at each interval stroke. Variation in the fatigue limits can be observed across test batches, but more notably, between the different manufacturers. The springs produced by manufacturer Y demonstrate slightly higher fatigue limits. This variation is likely due to the differences in surface finishing processes between the two manufacturers, however a greater volume of testing data is required for each spring and design. Given that the previous loading cycles at a lower stroke do not influence the oscillatory loading at the subsequent stroke tested, the latter completed tests could be initiated at higher strokes once the approximate failing limit range was ascertained. This is the reason why some of the tests start at higher strokes, e.g. design A manufacturer Y in Figure 3. The 'x' indicates when failure occurred. Spring design A manufacturer Y was retained as the selected spring for the passive displacer given the higher fatigue limit demonstrated.

EXPERIMENTAL TESTING

The passive displacer experimental assembly is shown in Figure 5, where the passive displacer was incorporated into the SPTC warm end. An optical window was installed at the backend and

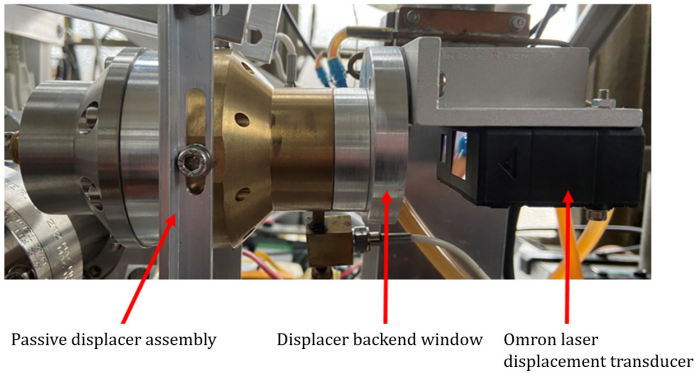

Figure 5. The passive displacer testing setup, installed into the coaxial Stirling pulse tube cryocooler at the warm end.

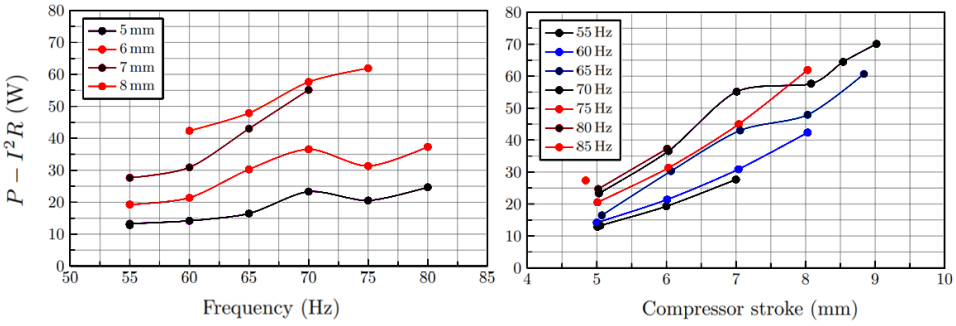

Figure 6. Compressor performance while displacer is clamped.

Table 1. Dynamic test inputs and the resulting displacer activity.

Test conditions	Input value	Result	Output value
f	55 Hz	x_d	3 mm
P_{fill}	30 bar	ϕ_d	72°
T_c	250 K	Q_c	1.6 W
x_c	7 mm		
Sampling rate	5000 s^{-1}		

an Omron laser displacement transducer was aligned with the displacer piston in order to measure in-situ displacement of the displacer during cryocooler operation. The latter displacement measurement tool was used in place of the contact probe (which was part of the original design as can be seen in Figure 2) as it was found to be more effective.

DISPLACER VALIDATION

Clamped Displacer

Figure 6 presents the compressor performance which was assessed during SPTC operation whilst the displacer was clamped. An increase in compressor stroke and frequency (input drives) resulted in an increase in compressor shaft power with varying optimums. This indicates normal operation of the compressor prior to investigating the passive displacer activity.

Dynamic Test

A dynamic test of the full SPTC was run with the inputs as given in Table 1. Whilst the SPTC in question has been designed for a cold temperature of 80 K, cooling was not required for validating the displacer dynamics and hence the test was run at $T_c = 250$ K. The resultant operation of the SPTC is further shown in Table 1, where an input compressor stroke x_c of 7 mm results in a passive displacer stroke x_d of 3 mm and a displacer phase ϕ_d of 72°. The fill pressure and compressor drive frequency were 30 bar and 55 Hz respectively. The pressure was measured at either end of the displacer using pressure transducers and the displacement was continuously measured using the Omron laser displacement transducer, as shown in Figure 5.

Figure 7 shows the harmonic and pressure forces acting on the displacer during the dynamic test. The displacement x_d and pressure P were reconstructed as per Equations 1 and 2. The inlet, PT and body pressure forces, as expressed in Equation 3, have been summed to produce a total pressure force driving the displacer. Similarly, the displacement, damping and inertial forces, as expressed

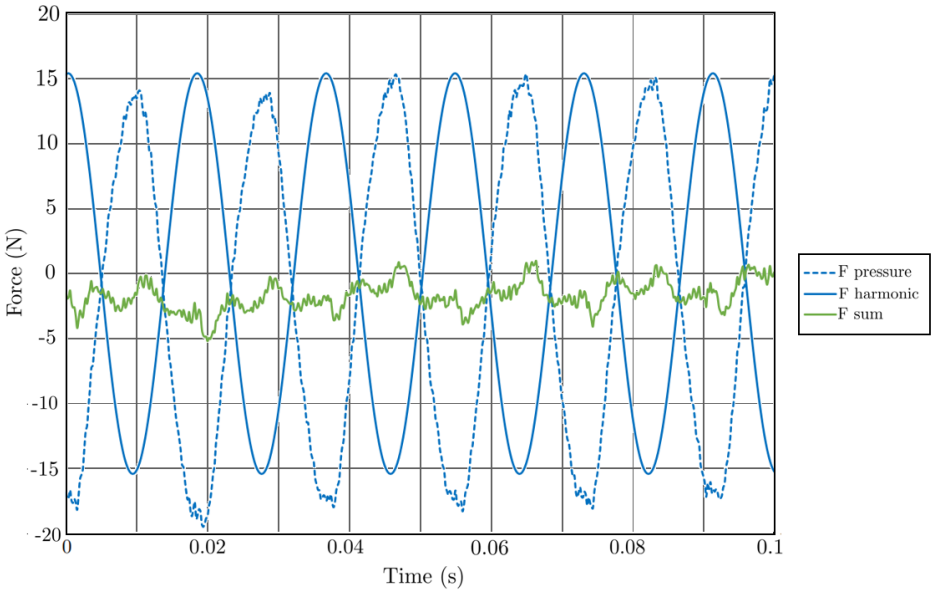

Figure 7. Pressure and harmonic forces driving the displacer.

in Equation 3, are summed to give a total harmonic force for the displacer. The forces are shown to act in balance with a 180° phase difference and this corroborates the design performance.

SUMMARY

In summary, a physical passive displacer has been designed, built and tested. Key components influencing the harmonic design were experimentally investigated; most significantly, the flexure springs were fatigue tested in order to select the most appropriate design for use in the passive displacer. A suitable experimental setup for the passive SPTC operation has been assembled and the passive displacer dynamic activity has been experimentally validated, where the harmonic and pressure forces driving the displacer permit it to run passively. The next steps include investigating the performance of the full SPTC at the design cold temperature of 80 K and comparing the performance with that of the active displacer SPTC.

ACKNOWLEDGEMENTS

The authors would like to acknowledge partial funding from the EPSRC with EP/N017013/1 and Honeywell Hymatic for this project and broader SPTC research within the Cryogenic Engineering group at the University of Oxford. Furthermore, they would like to thank the reviewers of *Cryocoolers*.

REFERENCES

1. Radebaugh, R., "Thermodynamics of regenerative refrigerators," *Generation of Low Temperature and its Applications*, (2003), pp. 1-20.
2. Rana, H., et al., "Numerical modelling of a coaxial Stirling pulse tube cryocooler with an active displacer for space applications," *Cryogenics*, vol. 106 (2020).
3. Abolghasemi, M. A., et al., "Coaxial Stirling pulse tube cryocooler with active displacer," *Cryogenics*, vol. 111 (2020).
4. Zhu, S., Nogawa, M., "Pulse tube Stirling machines with warm gas-driven displacer," *Cryogenics*, vol. 50, no. 5, (2010).

5. Rana, H., et al., "A passive displacer for a Stirling pulse tube cryocooler," *Cryocoolers 21*, ICC Press, Boulder, CO (2021).

6. Bailey, P.B., et al., "Low cost flexure spring testing," *IOP Conference Series: Materials Science and Engineering*, vol. 502 (2019).